Materials Research. 2015; 18(2): 250-257
DOI: http://dx.doi.org/10.1590/1516-1439.283214

Effect of Specimen Size on the Resistance to Thermal Shock of Refractory Castables Containing Eutectic Aggregates

Dan Yushin Miyaji[a]*, Caio Zuccolotto Otofuji[a], Antonio Henrique Alves Pereira[a], José de Anchieta Rodrigues[a]

[a]Universidade Federal de São Carlos – UFSCar, Rodovia Washington Luís, km 235, CEP 13565-905, São Carlos, SP, Brazil

Received: April 4, 2014; Revised: February 12, 2015

Thermal shock is one of the most severe conditions to which a refractory lining can be subjected to during its industrial application. Thus, there are several methods available for testing thermal shock damage resistance of refractories. Among them, a very common method is the quench test, which consists of quenching a hot refractory bar into water. After that a retained mechanical property is determined. Considering this, the aim of the work herein is to compare the thermal shock damage resistance between two specimen sizes among several materials. The dimensions 150 mm × 25 mm × 25 mm and 160 mm × 40 mm × 40 mm were used. The small bars are generally used for mechanical characterization in the refractory field (recommended by ASTM C1171-05). The large bars, on the other hand, are a requirement of DIN 196-1, which regards procedures for testing cement materials. Experimental results have indicated that the thermal shock damage is bigger for the large bars, as predicted by theoretical aspects. Although the size difference between the specimens was not so big, it was possible to observe the size effect using a statistical treatment. Five different castable formulations, of which three contained eutectic aggregates, were tested. The highest variation found in thermal shock damage resistance because of the size was about 15%.

Keywords: *thermal shock, refractory castables, eutectic aggregates, size effect*

1. Introduction

The most interesting aspect of the investigation of specimen size effects on the thermal shock damage resistance of refractories is the better understanding of the variables related to the quench test. Although literature[1-3] has provided solutions about this issue, it is sometimes neglected by refractory researchers and users. Such aspect has been given emphasis in the work herein.

It is well known that, during a thermal shock test, the larger the volume of a specimen, the higher the thermal gradient in it. This is because Biot modulus is directly proportional to the thickness. Yet, according to Cotterell et al.[1], mechanical size effects can also influence the thermal shock damage resistance of specimens. This issue was first pointed out in refractories by Kienow[2].

In the refractory field, the most common dimensions of laboratorial specimens are 150 mm × 25 mm × 25 mm. They are a recommendation of ASTM C1171-05[4] (Standard Test Method for Quantitatively Measuring the Effect of Thermal Shock and Thermal Cycling on Refractories). The dimensions of 160 mm × 40 mm × 40 mm have been taken as an interesting choice for the work herein as they are also a standardized dimension[5] (mechanical tests for cementitious materials from DIN). The mechanical behavior of the materials presented forward was evaluated for the both specimen sizes.

*e-mail: dan.miyaji@gmail.com

Actually, the differences in specimen's dimensions chosen for this work are not big enough to observe a large difference in the thermal shock damage resistance of refractories. This is the reason why a rigorous statistical procedure was applied to guarantee the size effect observation.

The authors believe that the work herein is relevant for the awareness of refractory users. According to them, users should consider possible brittle behavior transition of the large components in the industrial equipment in comparison to the small laboratorial specimens.

1.1. The mechanical size effect

Prior to describing the mechanical size effect on the resistance to thermal shock damage of specimens, it is necessary to present the relation given by the non-dimensional depth (bar thickness), $\overline{W}$[1]. The equation below shows that relation:

$$\overline{W} = \frac{W}{L_{CH}} \quad (1)$$

where W is the specimen depth (thickness) and L_{CH} is the characteristic length[6]. Equation 1 is somewhat similar to the so called "brittleness number", B, which is a classic parameter recently addressed in a work by Bradt & Harmuth[7]. The characteristic length, L_{CH}, is related to some mechanical properties of a material. They are the specific

fracture energy, G_F; the Young's modulus, E; and the tensile strength, σ_f. The equation of L_{CH} is presented below:

$$L_{CH} = \frac{G_F \cdot E}{\sigma_f^2} \quad (2)$$

Equation 1 shows that $\overline{W}$ relates spatial dimension (W) to materials properties. It is known that the higher the $\overline{W}$, the more brittle the fracture behavior tends to be in a specimen that is stressed to catastrophic failure. Here, brittleness can be defined as the tendency of a crack to propagate unstably, after its initiation. Therefore, based on Equation 1, there are two ways to increase the brittle stress of a specimen. It can be achieved by reducing L_{CH} or increasing W, or both concomitantly.

Actually, the term L_{CH} contains considerable information about the brittle behavior of a material by itself. The larger this value gets, the higher is the expected toughness. Moreover, the unit of L_{CH} is a length, whose value is comparable to the size of the Fracture Process Zone (FPZ) of a crack in a material[8].

Interestingly, L_{CH} appears to be very similar to the R""-parameter, presented by Hasselman[9,10], which is also known as a thermal shock damage resistance parameter. It is shown below:

$$R"" = \frac{\gamma_{WOF} \cdot E}{\sigma_f^2} \quad (3)$$

where γ_{WOF} is the fracture energy. Considering that $G_F = 2 \cdot \gamma_{WOF}$[7,11], it is evident the $L_{CH} = 2 \cdot R""$.

The meaning of R"" (and L_{CH}) is better understood by observing that it is directly proportional to the fracture energy and inversely proportional to the stored elastic strain energy. Fracture energy can be defined as the amount of energy that is necessary to generate a crack surface in a material per unit of projected area. However, the complete understanding of Equations 2 and 3 depends on clarifying the meaning of the ratio E/σ_f^2. Beforehand, though, it is necessary to consider the classical Griffith equation[12,13], which is presented below:

$$\sigma_f = \sqrt{\frac{2 \cdot E \cdot \gamma_{EFF}}{\pi \cdot c}} \quad (4)$$

where c is the crack length and γ_{EFF} is the effective surface energy, which can be defined as the energy per unit of area necessary for fracture at atomic level, plus some microplastic deformation.

The Griffith equation describes the conditions needed for the occurrence of a catastrophic and brittle fracture for a plate-like specimen, with a perforating elliptical flaw of length 2c. If c is isolated in the Equation 4, one would have:

$$c = \frac{\gamma_{EFF}}{\pi \cdot \frac{\sigma_f^2}{2 \cdot E}} \quad (5)$$

At this point, it is convenient to show that the ratio $\sigma_f^2/(2 \cdot E)$ can be interpreted as the elastic strain energy per unit of volume that is stored in a perfect brittle linear elastic specimen, which is subjected to a catastrophic failure in a pure tensile test. The area under the curve in Figure 1 depicts this relationship.

In Equation 5, it is possible to take c as the ratio between the energy necessary to create a surface of 1 m^2, at the beginning of propagation, and the elastic energy stored per unit of volume (1 m^3) due to mechanical stress at the moment of fracture. Considering the similarity between Equations 2, 3 and 5, L_{CH} and R"" can be both understood as the ratio proportional to the fracture energy per the availability of elastic strain energy stored in the specimen. Subsequently, it becomes evident that the thermal shock damage resistance of a material can be improved by increasing fracture energy and/or reducing its capacity to store elastic energy.

Returning to Equation 1, the reader may still find difficult to visualize how size effects may affect the thermal shock damage resistance of a specimen. Mathematical predictions, by Cotterell et al.[1], clarify this relation, as presented in Figure 2. It shows the non-dimensional stress intensity factor $\overline{K}$ as a function of the normalized crack length, c_n, for a hot prismatic bar, when it is submitted to a thermal shock at a critical temperature. The equation of $\overline{K}$ is shown below. The parameter c_n is obtained by dividing the pre existing crack lengh, c, by W ($c_n = c/W$). An arrow in Figure 2 indicates the dependence of $\overline{K}$ and c_n on the non-dimensional time. The equation of non dimensional time, $\bar{t}$ is also shown below[1]

$$\overline{K} = \frac{K}{E \cdot \alpha \cdot \Delta T \cdot \sqrt{W}} \quad (6)$$

$$\bar{t} = \frac{k \cdot t}{\rho \cdot c \cdot W^2} \quad (7)$$

where t is time; k is thermal conductivity; ρ is the density; c is specific heat; K is the stress intensity factor at crack tip;

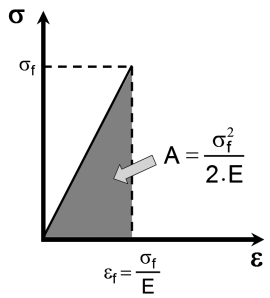

Figure 1. Stress-strain curve of a perfect brittle linear elastic specimen submitted to a catastrophic failure.

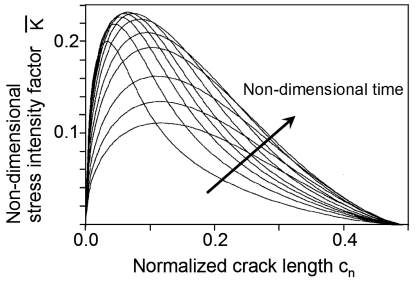

Figure 2. Non-dimensional stress intensity factor as a function of the normalized crack length. The arrow indicates the direction of the non-dimensional time. This graph was adapted from the work of Cotterell et al.[1].

α is the coefficient of linear thermal expansion; ΔT is the thermal shock temperature differential.

The mathematical deduction of $\overline{K}$ is well explained by Cotterell[1] and it will not be presented again here. In the present context, $\overline{K}$ has basically the same meaning of the stress intensity factor K.

The specimen geometry related to Figure 2 is a prismatic bar that contains a surface crack with a straight front. The use of non-dimensional and/or normalized values brings a generalist aspect to this subject, in a way that relations and/or ratios are more important than absolute values or dimensions.

Based on Figure 2, the following is the essential analysis needed in this study: basically two regions in the graph must be observed, which are the areas at the left of the maximum point (maximum of the maxima) and at the right of it. The values of $\overline{K}$ and c_n at the maximum of the maxima are 0.23 and 0.065, respectively, at a non-dimensional time of 0.005.

Therefore, if a specimen is submitted to thermal shock and c_n is lower than 0.065, crack propagation will be unstable. This is so because $\overline{K}$ values increase as a function of c_n, and also as a function of non-dimensional time. On the other hand, if c_n is higher than 0.065, the crack growth will be stable under thermal shock.

Further deductions made by Cotterell et al.[1] on this issue come to a simplified criterion. If $\overline{W} > 3.9$, a highly unstable crack propagation would be observed in a specimen submitted to thermal shock. On the contrary, stable crack propagation would occur for $\overline{W} < 3.9$. Adding to that, when $\overline{W} = 3.9$, it represents the situation in which coordinates c_n and $\overline{K}$ (in Figure 2) correspond to the point of maximum of all maxima.

It has to be noticed that the graph in Figure 2 is based on models of Linear Elastic Fracture Mechanics, LEFM[12,13]. In the context of refractory ceramics, a refractory specimen would probably not behave exactly such as Figure 2 shows. This is so because the phenomenon of crack propagation for refractories is better represented by a fracture process zone than it is by a non-linear single crack with a straight front. Thus, each material will react in their own peculiar way, once toughening mechanisms depend mostly on the microstructure of the materials.

Nevertheless, a change in the brittle behavior because of mechanical size effects is still expected for materials with a complex fracture process zone[1]. The major difference is, probably, that for very linear materials (for instance, structural technical ceramics), the transition between a more brittle to a less brittle behavior would be more evident (the point of maximum of maxima). In the case of refractories, which are highly non-linear materials, such a transition might be gradual, or not easily detectable.

Bažant[14,15] intensely investigated size effects in building materials and an argument presented by him also aids the understanding of size effects. If one assumes that γ_{WOF} is a function of the size of process zone, the crack length, c, can be obtained from this relation. For very large structures, it can be assumed that $W \rightarrow \infty$ and c becomes too small compared to W. Therefore, γ_{WOF} is not expressive to halt crack propagation (relatively, R-curve behavior becomes small). Thus, linear fracture mechanics is applicable for this situation, where crack propagation must occur unstably. On the contrary, for a small bar made of this material where the size of process zone is close to W, crack propagation should occur less unstably and linear fracture mechanics is not applicable. In other words, size effects may strongly interfere. For instance, big differences in dimensions of specimens may present disparity in the brittle behavior among them.

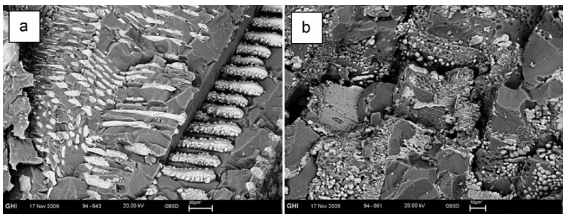

Figure 3. Fractographies by SEM of eutectic electrofused aggregates: a) mullite-zirconia[16] b) alumina-zirconia.

1.2. Castables containing electrofused eutectic aggregates

Eutectic microstructures tend to present a complex configuration of 2 or more phases. Furthermore, such microstructures have a large number of interfaces. Fractographies of eutectic aggregates of mullite-zirconia and alumina-zirconia, obtained for the present work, are shown in Figure 3.

Previous work[17] has indicated that the addition of eutectic mullite-zirconia or alumina-zirconia aggregates to refractory castables can enhance their fracture energy significantly, and improve their resistance to thermal shock as well. As a result, higher values for R"" were obtained, which would also result in low values of $\overline{W}$. In that case, castables containing eutectic aggregates may be expected to be less susceptible to variations in thermal shock damage resistance caused by size effects. This aspect was investigated and the results are presented in the following sections.

2. Material and Methods

2.1. Castables formulation and processing

Five castable formulations were designed for the present work. They followed Andreasen's particle packing model with the q = 0.26. Two maximum aggregate sizes were used, one of 2.3 mm and the other of 8.0 mm. Further information of each formulation is presented in Table 1.

In Table 2 the complete list of used raw materials is presented with their correspondent range of particle size. The matrix particles of all castables used consisted of the three materials: Elfusa-TP200, Almatis-CL370 and Almatis-CT3000SG. Calcium aluminate cement (EL61, from Elfusa) was added, whose amount represents 4% of total mass. Citric acid were used as dispersant and as curing retardant, and the correspondent amount was 0.05% of formulation total mass.

It must be noticed in Table 1 that the amount of aggregates in castables A8 and M8 is different from the one of A2, M2 and Z2, and an explanation of this fact is given herein for convenience. First it must be defined the term "matrix", which corresponds to the particles with sizes $d \leq 100$ μm. As the range of accumulated volume or particles with

Table 1. Formulation of the five refractory castables.

	Maximum aggregate size (mm)	Aggregate amount (wt-%)	Eutectic aggregate amount (wt-%)	Aggregate type
A8	8.0	67.0	0.0	Electrofused white alumina
M8	8.0	67.0	31.0	Electrofused eutectic mullite-zirconia
A2	2.3	58.0	0.0	Electrofused white alumina
M2	2.3	58.0	22.0	Electrofused eutectic mullite-zirconia
Z2	2.3	58.0	22.0	Electrofused eutectic alumina-zirconia

Table 2. Raw materials used in the formulation of the castables ("FX"-type materials were a courtesy of ELFUSA. CL370 and CT3000SG were a courtesy of Almatis).

Raw materials	Particle diameter range (μm)
a) FX 5/16*	$8000 \geq d > 4000$
b) FX 4/10*	$4750 \geq d > 1700$
c) FX 8/20*	$2360 \geq d > 710$
d) FX 8MF	$2360 \geq d > 125$
e) FX 10/36*	$2000 \geq d > 355$
f) FX 20/40	$855 \geq d > 355$
g) FX 40MF	$425 \geq d > 90$
h) FX 60MF	$250 \geq d > 16$
i) FX TP200	$212 \geq d > 16$
j) CL 370	$d_{average} = 3.1$
k) CT 3000SG	$d_{average} = 1.4$

*raw materials available as white electrofused alumina or mullite-zirconia or alumina-zirconia. "a" to "i" correspond to Elfusa S.A.; "j" and "k" correspond to Almatis.

$d > 100$ μm is larger for castables A8 and M8, once their maximum aggregate size is 8.0 mm, consequently those castables must have large amount of aggregates than A2, M2 and Z2, whose maximum aggregate size is 2.3 mm. This is because the particle size distribution is kept constant among all formulations. In other words, two formulations with different maximum aggregate size in relation to each other will only have equal amount of aggregates (volume or particles with $d \geq 100$ μm) if they have different particle size distribution.

Sintering was carried out at 1450 °C for 10 hours, under a heating rate of 3 °C/min, in a furnace of the brand Lindberg (type Blue M, in air, or non-controlled atmosphere). The cooling of specimens to room temperature inside of the furnace was proceeded under a rate of 10 °C/min.

It is important to note that the castables M2 and Z2 were obtained based on the formulation of castable A2. It was done by replacing the largest particles of A2 by another of eutectic ones. The same procedure was followed in order to obtain M8, whose reference material is A8.

All castables were mixed with 4.8 to 5.0 wt-% of water, so that the free flowing (FF) property of A2, M2 and Z2 were about 20%, and their vibrated flowing (VF) was 130%. For A8 and M8, FF was 0% and VB was 135%.

2.2. Thermal shock tests and the characterization of Young's modulus and modulus of rupture

As aforementioned, the bar dimensions chosen for the work herein were 150 mm × 25 mm × 25 mm (small bars), and 160 mm × 40 mm × 40mm (large bars).

For the characterization of thermal shock resistance of the small bars, 5 bars per castable composition were prepared. The bars were put 2 by 2 in a furnace previously heated at 825 °C. After a dwell time of 25 minutes for thermal stabilization, the bars were quenched into circulating water at 25 °C. In the case of the large bars, 3 bars per composition were prepared. Their quench tests were completed out using 1 bar at a time in the hot chamber, and each bar was kept there for 60 minutes for thermal stabilization. Only 1 thermal cycle was applied to each.

Young's modulus, E, of the specimens was measured in the equipment called Sonelastic (from ATCP-Engenharia Física, Brazil), which is in agreement with the ASTM E1876-09[18] requirements. This standard describes Young's modulus as a dynamic characterization based on the impulse excitation technique. It is a non-destructive characterization technique that was first applied by Coppola & Bradt[19] to refractories. By measuring the E-value of the specimens before and after the thermal shock, the parameter retained-E was measured. It is the ratio between the E-value after and the one before thermal shock, times 100.

For the characterization of the modulus of rupture, MOR, experimental procedures described in ASTM C133-97[20] were applied. The retained-MOR was determined by the ratio between the MOR after and the one before thermal shock, times 100.

2.3. Statistical tests

A software called PAST[21] was used to verify if numerical data groups presented statistical differences from each other. The "one-way-ANOVA" (analysis of variance) test was applied to analyze the statistical similarity between two average values. The null hypothesis was assumed if two average values were considered statistically equal. In that case, the significance level, p, must be higher than 0.05. To compare the statistical difference between average values among various groups of data (in that case, among A8, M8, A2, M2 and Z2), the two-way-ANOVA test was applied. In other words, the test was used to verify if a treatment was effective between two groupings (if a set of materials shaped in large specimens presents higher thermal shock damage than the smaller ones). The same significance level, p, previously mentioned, was assumed to verify the null hypothesis.

The specific interest in applying such statistical tests were for a correct analysis of R""-parameter (therefore L_{CH}), retained-E and retained-MOR. Because these parameters are often calculated from the average E, average MOR (and average γ_{WOF} for the case of R""), no numerical data group is produced. Thus, the proposed statistical tests are not possible. In the present work, this problem was solved by combining

results from each individual test to generate a variety of retained-MOR and retained-E values. This procedure is "data replication" and excludes any repeated combination. Figure 4 exemplifies how the data group of retained-MOR of the small bars was obtained for one castable.

As five tests were performed to obtain an average value of MOR for a single material, each test was numbered from one to five, and therefore named as "MOR1" to "MOR5". For the other set of five specimens (of the same material) submitted to thermal shock, the same procedure was followed, but named as "MOR1 TS" to "MOR5 TS".

According to the definition of "retained-MOR" given in the end subsection "statistical tests", each of MOR obtained for each specimen after thermal shock was combined to each result of MOR before thermal shock. Therefore, the ratio $\frac{\text{MOR 1 TS}}{\text{MOR 2}}$ x100 has been calculated and named as "retained-MOR **1-1"**. Likewise, "retained-MOR **1-2"** corresponds to the ratio $\frac{\text{MOR 1 TS}}{\text{MOR 1}}$ x100. If one obtains the whole sequence from retained-MOR **1-1** to retained-MOR **5-5**, there will be 25 values involved, which are sufficient for applying the statistical tests. The same data replication technique was also used to obtain the data groups for retained-E for all specimen sizes.

3. Results and Discussion

Before presenting the main discussion regarding this work, it is important to analyze the values of MOR and E of the bar-like specimens with different W-values. They can be seen in Table 3.

Two general tendencies can be observed in the data shown in Table 3. The first is, for materials with similar chemical composition, the increasing in aggregate size caused lower modulus of rupture and Young's modulus. This fact is probably related to the phenomenon of the thermal expansion anisotropy[22] during the sintering of these materials. The another tendency is the following: by comparing castables with similar maximum aggregates sizes, it is noticed that the replacement of white electrofused alumina aggregates by eutectic ones also lowered the mechanical resistance. In this case, the difference in linear thermal expansion coefficient between the different phases, during sintering, is the most probable cause for the occurrence of defects in the material.

Furthermore, Table 3 indicates that the large specimens presented lower average MOR-values than the small bars. If a Weibull-parameter[13] of 1 to 5 (reasonable for refractories) is assumed, it means that the MOR of the large specimens must have decreased about 32% to 80%. Consequently, processing conditions to produce the large bars seem not to increase significantly the concentration and size of defects in them.

In Figure 5, the large specimens did not show any differences in retained-E after thermal shock, except for A2, which showed higher thermal shock damage for the case W = 40 mm than it did for W = 25 mm. The one-way-ANOVA test confirmed that, in fact, only A2 presented a statistical significance difference ($p < 0.05$) for the average values of E between W = 40 mm and W = 25 mm.

The retained-MOR (Figure 6) of the specimens with W = 40 mm has presented a higher thermal shock damage than the ones with W = 25 mm. However, the error bars in each material group clearly overlaps, which causes an uncertainty when distinguishing the values from each other.

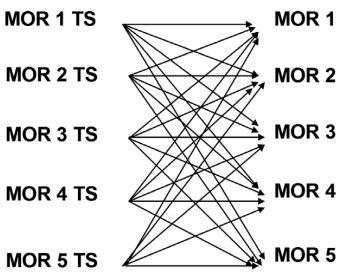

Figure 4. Generation of a data group of retained-MOR for the small bars by combining individual MOR-values results before and after thermal shock test. The term "TS" refers to the values of MOR after thermal shock.

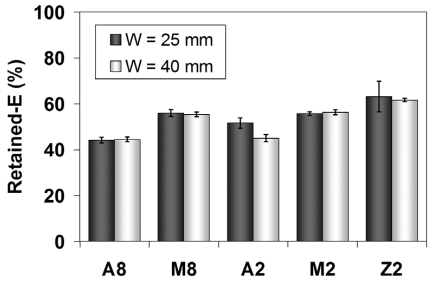

Figure 5. Retained-E of the refractory castables after thermal shock of ΔT = 800 °C for small and large specimens.

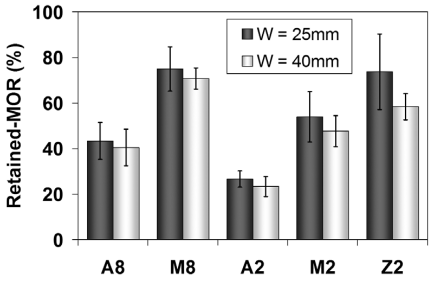

Figure 6. Retained-MOR of the refractory castables after thermal shock of ΔT = 800 °C for small and large specimens.

Table 3. Values of MOR and E of bar-like specimens of the castables for the two values of W.

	A8	M8	A2	M2	Z2
MOR (MPa), W = 25 mm	17.8±3.2	12.7±1.4	32.7±3.7	22.4±1.6	16.7±2.2
MOR (MPa), W = 40 mm	17.5±0.8	12.1±0.8	31.6±3.7	22.2±1.7	16.0±0.9
E (GPa), W = 25 mm	100.6±8.2	43.2±7.7	122.3±10.8	73.8±5.4	61.8±3.5
E (GPa), W = 40 mm	107.6±4.2	45.6±0.6	118.0±5.2	80.1±1.7	52.5±2.1

The one-way-ANOVA test applied to retained-MOR data groups has indicated that only A2 and Z2 present significant statistical differences between specimens with W = 40 mm and W = 25 mm.

However, it must be considered that all average values of the retained-MOR depicted in grey bars (Figure 6) are lower than the correspondent dark bars for each castable. Thus, to confirm if the specimens with W = 40 mm have a decreasing tendency of their retained-MOR, the "two-way-ANOVA" test was applied. The result for p was extremely low (0.000032), which indicates statistical significance. Literally, this statistical test shows that the thermal shock has a different response on the retained-MOR for specimens with W = 40mm when compared to W = 25mm. In other words, the specimens of higher volume most probably have lower resistance to thermal shock damage than the smaller bars.

Because there was no significant difference in the values of E and MOR among specimens with different W (right after the sintering; Table 3), the values of $\overline{W}$ determined to specimens with W = 40 mm must be higher than the ones with W = 25mm. This is shown in Figure 7, in which the inverse of $\overline{W}$ ($1/\overline{W}$) is depicted in a bar graph to facilitate the comparison with other figures (the analysis of the inverse of $\overline{W}$ makes comparison graphically easier). Other necessary data to determine $\overline{W}$ is presented in Table 4, in addition to E and MOR values aforementioned in Table 3.

The initial expectation was that there is a direct relation between the thermal shock damage resistance and $1/\overline{W}$. As the retained-E was not sensitive to the variation of W, such relation is better given by the values of retained-MOR. This result is very important, because, although E and MOR are properties that represent the integrity of the material, they may not always show the same trend. In that case, the MOR seems to be more affected by size effects than E after the thermal shock.

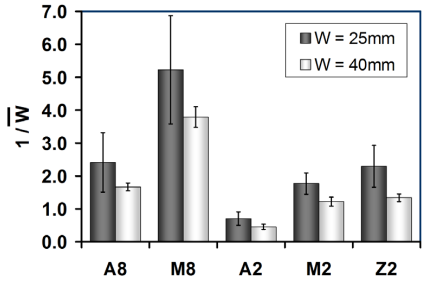

Figure 7. Comparison of $1/\overline{W}$ among all castables of this work.

Another interesting observation is that specimens with W = 40 mm aided to distinguish the resistance to thermal shock between M8 and Z2, which was not possible by comparing results obtained from specimens with W = 25mm.

The initial expectation that the eutectic aggregate containing castables would be less susceptive to mechanical size effects is not confirmed, once retained-MOR of Z2 varied more than the one of A2. A possible explanation for that could be the fact that the fracture process zone length of all specimens is too close to W. Although size effects are evident and have influenced thermal shock damage resistance, it is still not enough to obtain precise proportionality between $\overline{W}$ and retained-MOR.

All analysis performed in the present section assumed that the higher thermal shock damage observed for the large specimens is a consequence of a mechanical size effect. As no additional tests were made concerning the thermal properties, the next section discusses how much the thermal properties may have influenced the resistance to thermal shock damage due to the change of W.

3.1. Estimating the Biot modulus

In order to estimate the Biot modulus, the most important property to be evaluated for the present work is the thermal conductivity, k. Based on the work of Akiyoshi et al.[23], a castable with chemical and mineralogical compositions similar to A2 and A8 (with porosities of about 14%), would present a k-value close to 2.5 W/(m·K). Akiyoshi's paper reports an investigation for predicting the thermal conductivity of alumino-silicate refractories. The equation to calculate the Biot modulus, β, is the following[1,3]:

$$\beta = \frac{W \cdot h}{k} \quad (8)$$

where h is the heat transfer coefficient. For this specific case, it was considered h = 10.000 W/m^2, which is adequate for the thermal shock of specimens dropped into circulating water.

In Table 5, the values of Biot modulus for A2 and A8 were estimated by assuming k = 2.5 W/(m·K) with an error of ±0.5 W/(m·K).

According to Cotterell et al.[1] the condition β > 100 is enough for the temperature on the specimen's surface to equalize instantaneously with the one of the quenching medium, during the thermal shock. Therefore, if an increase in the thermal gradient level is not supposed to happen for β above 100, a higher thermal shock damage because of an increase in W would be a consequence of an enhancement in the inherent brittleness.

Table 4. γ_{WOF}, R'''' and L_{CH} of bar-like samples, considering the two values of W for all castables.

	A8	M8	A2	M2	Z2
γ_{WOF} (J/m^2)	95±5	243±32	77±12	151±13	130±8
R''''(m) W = 25 mm	0.030±0.011	0.063±0.020	0.009±0.003	0.022±0.004	0.029±0.008
R'''' (m) W = 40 mm	0.033±0.004	0.076±0.010	0.009±0.003	0.024±0.004	0.027±0.004
L_{CH} (m) W = 25 mm	0.060±0.022	0.126±0.040	0.018±0.006	0.044±0.008	0.058±0.016
L_{CH} (m) W = 40 mm	0.066±0.008	0.152±0.020	0.018±0.006	0.048±0.008	0.054±0.008

Table 5. Biot modulus estimative for materials A2 and A8.

	W= 25 mm	W= 40 mm
β for k= 2.0 W/(m·K)	125.0	200.0
β for k= 2.5 W/(m·K)	100.0	160.0
β for k= 3.0 W/(m·K)	83.0	133.0

Table 6. Thermal conductivity of dense oxides.

Oxide	Thermal conductivity
Alumina with 99% purity, density 3.96 g/cm^3	33.0 W/(m·K)
Mullite, density 2.80 g/cm^3	3.5 W/(m·K)
Zirconia, density 5.68 g/cm^3	1.7 W/(m·K)

Looking at the data on Table 5, a value of k of about 2.5 W/(m·K) results in a Biot modulus high enough to fulfill the criterion suggested by Cotterell et al.[1], for W ≥ 25mm. However, there is an interference of thermal aspects for values of k ≥ 2.5 W/(m·K). In other words, if a k-value of 3.0 W/(m·K) is assumed as the thermal conductivity of A8 and A2, there is no certainty that mechanical size effects are the cause of a higher thermal shock damage in specimens with W = 40 mm.

No estimation of k was done for M8, M2 and Z2. However, their k is most probably lower than those of A8 and A2. This is so because dense mullite and zirconia have a lower thermal conductivity than the dense alumina. This hypothesis can be confirmed by a simple application of the volume-fraction rule[3,24]. Table 6 shows the thermal conductivity of dense alumina, mullite and zirconia[25].

3.2. Final remarks about the size of the specimens

The obtained results confirm the theoretical expectation given by Cotterell et al.[1]. Therefore, thermal shock damage resistance characterization can be more precise when using specimens of large volumes. Among the two sizes studied herein, the dimensions of 160 mm × 40 mm × 40 mm are recommended.

Although size effects were clear (by means of an adequate statistical test) in the work herein, they may not be considered relevant because the differences in the thermal shock damage resistance were small. For instance, if refractory thermal insulators had been chosen for experiments, size effects would have probably been undetectable. This would happen because σ_f of insulator is usually low, resulting in high values of L_{CH} and low values of $\overline{W}$. The two specimen sizes chosen in the work herein are very close, being that the main reason for the small differences found.

Nevertheless, it is considered that the obtained results are important for the awareness of refractory researchers and users regarding possible differences in the material's behavior between laboratorial tests and practical situations in industries. Components of very large sizes or big volumes, much bigger than the specimens mentioned in this work, are frequently employed in industries. Considering this, the transition to the brittle behavior will certainly happen.

Additionally, the size effect may also become more evident as the modulus of rupture of materials increases. That is the tendency observed in the refractory area nowadays. In that case, attention is recommended.

4. Conclusions

Based on the investigations carried out in the present work, the following conclusions can be presented:

- The retained-E showed no change comparing small and large specimens when considering the thermal shock damage resistance of the castables containing eutectic aggregates, with maximum aggregate size of 2.3mm. The most resistant material in this sense was Z2, which retained about 61% of its original Young's modulus after a thermal shock of ΔT = 800 °C (into water).
- The retained-MOR indicated that the large specimens presented higher thermal shock damage than the small ones. However, castables containing eutectic aggregates were not less susceptible to size effects than the reference materials, as the initial expectation. The highest drop in thermal shock resistance due to size effects was presented by Z2, of about 15%.
- The best thermal shock damage resistant material was M8, which retained 70.4% of its initial MOR value (determined by large specimens).
- Larger specimens with higher volumes distinguished the resistance to thermal shock among the castables better.

Acknowledgements

The authors would like to acknowledge the companies Elfusa and Almatis for the donation of raw materials. The authors are also grateful to CNPq (budgets 141028/2008-4, 141868/2008-2, 155734/2010-5, 303061/2009-0 and 307127/2013-3). Additional thanks to Dr. Øyvind Hammer (Natural History Museum – Oslo – Norway) for helping on discussions about statistics.

References

1. Cotterell B, Ong SW and Qin C. Thermal shock and size effects in castable refractories. *Journal of the American Ceramic Society*. 1995; 78(8):2056-2064. http://dx.doi.org/10.1111/j.1151-2916.1995.tb08617.x.
2. Kienow S. Crack fromation in fired converter bricks. *Berichte der Deutschen Keramischen Gesellschaft*. 1970; 47(7):426-430.
3. Kingery WD, Bowen HK and Uhlmann DR. *Introduction to ceramics*. 2nd ed. New York: John Wiley & Sons; 1976.
4. American Society for Testing and Materials – ASTM. *ASTM C1171-05: standard test method for quantitatively measuring the effect of thermal shock and thermal cycling on refractories*. West Conshohocken; 2011.
5. Deutsches Institut für Normung – DIN. *DIN EN 196-1: methods of testing cement. Part 1: determination of strength*. German; 2005.
6. Peterson PE. Fracture energy of concrete: method of determination. *Cement and Concrete Research*. 1980; 10(1):79-89. http://dx.doi.org/10.1016/0008-8846(80)90054-X.

7. Bradt RC and Harmuth H. The fracture resistance of refractories. *Refractories World Forum*. 2011; 3(4):129-132.
8. Cotterell B. *Fracture and life*. London: Imperial College Press; 2010.
9. Hasselman DPH. Unified theory of thermal shock fracture initiation and crack propagation in brittle ceramics. *Journal of the American Ceramic Society*. 1969; 52(11):600-604. http://dx.doi.org/10.1111/j.1151-2916.1969.tb15848.x.
10. Hasselman DPH. Figures-of-merit for the thermal stress resistance of high-temperature brittle materials: a review. *Ceramurgia International*. 1978; 4(4):147-150. http://dx.doi.org/10.1016/0390-5519(78)90028-5.
11. Harmuth H. Stability of crack propagation associated with fracture energy determined by wedge splitting specimen. *Theoretical and Applied Fracture Mechanics*. 1995; 23(1):103-108. http://dx.doi.org/10.1016/0167-8442(95)00008-3.
12. Lawn B. *Fracture of brittle solids*. 2nd ed. Cambridge: Cambridge Press; 1998.
13. Wachtman JB. *Mechanical properties of ceramics*. New York: John Wiley & Sons; 1996.
14. Bažant Z and Planas J. *Fracture and size effect in concrete and other quasibrittle materials*. Boca Raton: CRC Press; 1998.
15. Bažant Z and Kazemi M. Size effect in fracture of ceramics and its use to determine fracture energy and effective process zone length. *Journal of the American Ceramic Society*. 1990; 73(7):1841-1853. http://dx.doi.org/10.1111/j.1151-2916.1990.tb05233.x.
16. Miyaji DY, Heuter H, Tonnesen T and Rodrigues JA. Fractography by SEM of eutectic electrofused aggregates of mullite-zirconia in refractory castables. In: 54th Brazilian Ceramic Conference; 2010; Foz do Iguaçu. Brazil. Associação Brasileira de Ceramica; 2010. CD-ROM.
17. Miyaji DY, Tonnesen T and Rodrigues JA. Eutectic aggregates containing refractory castables: what are the effects on fracture energy and thermal shock resistance? In: Proceedings of the Unified Technical Conference on Refractories; 2011; Kyoto. Japan. Technical Association of Refractories Japan; 2011. CD-ROM.
18. American Society for Testing and Materials – ASTM. *ASTM E1876-09: standard test method for dynamic young's modulus, shear modulus, and poisson's ratio by impulse excitation of vibration*. West Conshohocken; 2009.
19. Coppola JA and Bradt RC. Thermal shock damage in SiC. *Journal of the American Ceramic Society*. 1973; 56(4):214-218. http://dx.doi.org/10.1111/j.1151-2916.1973.tb12460.x.
20. American Society for Testing and Materials – ASTM. *ASTM C133-97: standard test methods for cold crushing strength and modulus of rupture of refractories*. West Conshohocken; 2008.
21. PAST. *Palentological Statistics*. Available from: <http://folk.uio.no/ohammer/past/>. Access in: 25/04/2012.
22. Krstic VD. Critical grain-size/preexisting flaw size relations in anisotropic brittle solids. *Journal of the American Ceramic Society*. 1983; 66(10):726-729. http://dx.doi.org/10.1111/j.1151-2916.1983.tb10538.x.
23. Akiyoshi MM, Silva AP, Silva MG and Pandolfelli VC. Condutividade térmica e sua correlação com a temperatura e a massa específica volumétrica de materiais refratários sílico-aluminosos e aluminosos. *Cerâmica*. 2001; 47(301):18-27. http://dx.doi.org/10.1590/S0366-69132001000100005.
24. Chawla KK. *Composite materials: science and engineering*. New York: Springer-Verlag; 1987.. http://dx.doi.org/10.1007/978-1-4757-3912-1.
25. Material Property Data. Available from: <http://www.matweb.com/>. Access in: 04/11/2012.